Coherent state approach to the interacting boson model: Test of its validity in the transitional region

I. Inci,[1] C. E. Alonso,[2] J. M. Arias,[2] L. Fortunato,[3] and A. Vitturi[3]

[1]*Institute of Science, Erciyes University, TR-38039 Kayseri, Turkey*

[2]*Departamento de Física Atómica, Molecular y Nuclear, Facultad de Física, Universidad de Sevilla, Apartado 1065, ES-41080 Sevilla, Spain*

[3]*Dipartimento di Fisica Galileo Galilei and INFN, Via Marzolo 8, IT-35131 Padova, Italy*

(Received 5 June 2009; published 29 September 2009)

The predictive power of the coherent state (CS) approach to the interacting boson model (IBM) is tested far from the IBM dynamical symmetry limits. The transitional region along the γ-unstable path from U(5) to O(6) is considered. Excitation energy of the excited β band and intraband and interband transitions obtained within the CS approach are compared with the exact results as a function of the boson number N. We find that the CS formalism provides approximations to the exact results that are correct up to the order $1/N$ in the transitional region, except in a narrow region close to the critical point.

DOI: 10.1103/PhysRevC.80.034321 PACS number(s): 21.60.Fw, 21.60.Ev

I. INTRODUCTION

The study of shape phase transitions in finite nuclear quantal systems has recently been the subject of many investigations [1,2]. Different models have been used to describe the dynamics of the many-body systems. In most cases, a key instrumental role in characterizing the phase transitions and the critical points is played by the energy surfaces and their behavior as a function of the number of particles. In the specific case of the approaches based on the interacting boson model (IBM) [3], the energy surfaces are constructed from the boson coherent states [4–6]. It is well known that in correspondence with the dynamical symmetries, the results obtained within the intrinsic formalism for a number of observables (such as excitation energies, $E2$ matrix elements, two-particle transfer matrix elements, etc.) coincide, in leading order in $1/N$ (with N the boson number), with the corresponding exact values obtained directly diagonalizing the boson Hamiltonian. The aim of this paper is to study the capability of the coherent state (CS) formalism to provide good results also outside (and far from) these situations. For this study, we have selected the U(5) to O(6) leg of the Casten triangle. The critical point along this path was studied by Iachello solving the corresponding Bohr equation [7] for an infinite square well in the β variable and obtaining what is known as the critical point symmetry $E(5)$ [8]. The same physical situation has been treated within the IBM [9,10].

The selected path is known to preserve the γ instability and is therefore characterized by excited bands in the β degree of freedom only. The results of our study show that all along the transitional path (except in a narrow region close to the critical point), the CS formalism still provides estimates for energy bands and transitions that describe the exact values with the same degree of accuracy as in the limiting cases [in our case, the O(6) vertex], namely, in leading order in $1/N$. It is important to note that next-to-leading order terms are not correctly calculated within the CS approach. Consequently, no finite-N effects can be extracted from this formalism, and one has to rely on other methods [11–14].

The paper has the following structure. In Sec. II, the transitional Hamiltonian used is presented and the formalism of the coherent states revised, including the proper kernels to project the states from the intrinsic to the laboratory frame. In Sec. III, explicit expressions for selected excitation energies and $B(E2)$ transition rates within the CS approach along the complete O(6)–U(5) transitional region are obtained. These are compared with the exact calculations for different N values. Finally, Sec. IV summarizes the main conclusions.

II. HAMILTONIAN AND COHERENT STATES

We will consider the spherical to deformed γ-unstable shape transition by using the Hamiltonian

$$H_B = x\hat{n}_d - \frac{1-x}{N}\hat{Q}\cdot\hat{Q}, \tag{2.1}$$

where $\hat{n}_d$ is the d-boson number operator, and

$$\hat{Q} = (s^\dagger \times \tilde{d})^{(2)} + (d^\dagger \times \tilde{s})^{(2)} \tag{2.2}$$

is the assumed boson quadrupole operator. With our choice of the Hamiltonian, we obtain for $x = 1$ the U(5) dynamical symmetry and for $x = 0$ the O(6) one. Note that for any value of x, the choice of the quadrupole operator leads to a Hamiltonian that preserves the O(5) symmetry, and spectra are therefore characterized by its degeneracies and characteristic band structures (and associated γ instability). As we know [1], the Hamiltonian (2.1) describes a second-order phase transition, with the critical point occurring at the critical value $x_c = (4N-8)/(5N-8)$. In Fig. 1, a schematic diagram presents the low-lying spectra in the O(6) and U(5) limits. The relevant quantum numbers L [angular momentum which labels the O(3) irreducible representations (irreps)] and τ or v [O(5) seniority which labels the O(5) irreps] in each limit are explicitly given. It should be noted that in the literature, v is used when working with the basis associated with the U(5) dynamical symmetry, while τ is written in the base associated with the O(6) dynamical symmetry. For these two limiting situations, exact analytic $B(E2)$ values for selected transition rates have been obtained [3]. Those studied in this paper are indicated explicitly in Fig. 1 beside the arrows of the corresponding transitions.

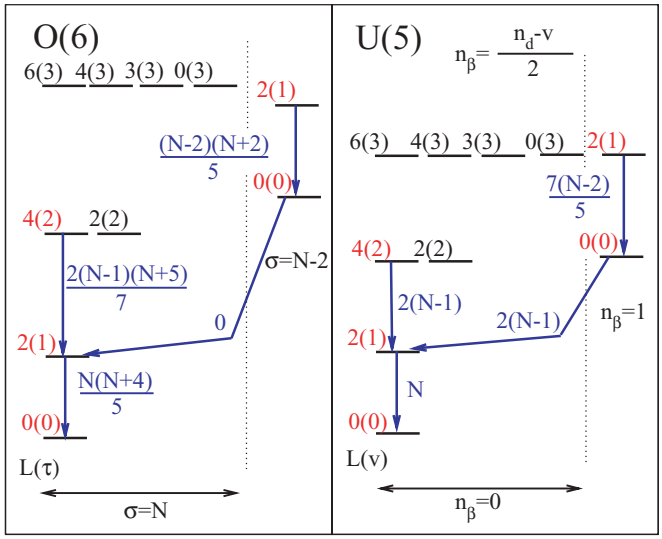

FIG. 1. (Color online) Schematic spectra for O(6) and U(5) dynamical symmetries. The states considered in this work in both cases are $L(v \text{ or } \tau) = 0(0), 2(1), 4(2)$ in the ground-state band [$\sigma = N$ in O(6) and $n_\beta = 0$ in U(5)] and $L(v \text{ or } \tau) = 0(0), 2(1)$ in the excited band [$\sigma = N-2$ in O(6) and $n_\beta = 1$ in U(5)]. Exact analytical $B(E2)$'s at the O(6) and U(5) limits for the transitions considered in this paper are explicitly given beside the corresponding arrows.

A. Exact calculations

The Hamiltonian (2.1) can be easily diagonalized with the method proposed in Ref. [10], even for large values of the number of bosons, N. The method provides the energies and the wave functions and, consequently, allows for the calculations of $B(E2)$ transition rates between initial $(\tau, L)_i$ and final $(\tau, L)_f$ states,

$$B\left(E2; \tau_i, L_i \to \tau_f, L_f\right) = \frac{1}{2L_i+1} |\langle \tau_f L_f || \widehat{T}^{E2} || \tau_i L_i \rangle|^2. \tag{2.3}$$

In the next section, we will present exact calculations using $\widehat{T}^{E2} = \widehat{Q}$, as given in Eq. (2.2), for the selected transitions along the U(5)–O(6) transitional region.

In addition, we will also consider the $E(0)$ transition from the 0^+ of the β band to the ground-state 0^+. The transition probability is associated with the matrix element of the operator $\hat{n}_s = N - \hat{n}_d$, i.e.,

$$B(E0; 0^+_\beta \to 0^+_g) = |\langle 0^+_g | \hat{n}_s | 0^+_\beta \rangle|^2. \tag{2.4}$$

B. Coherent state approach

A useful way of looking at phase transitions is to resort to the concept of intrinsic states and the associated energy surfaces. In the IBM for even nuclei, one introduces a ground-state intrinsic state of the form

$$\Phi_{\text{g.s.}}(\beta,\gamma) = \frac{1}{\sqrt{N!}} (b^\dagger_{\text{g.s.}}(\beta,\gamma))^N |0\rangle, \tag{2.5}$$

where the basic boson is given in the form

$$b^\dagger_{\text{g.s.}}(\beta,\gamma) = \frac{1}{\sqrt{1+\beta^2}} \left(s^\dagger + \beta \cos\gamma d^\dagger_0 + \frac{\beta}{\sqrt{2}} \sin\gamma (d^\dagger_2 + d^\dagger_{-2}) \right), \tag{2.6}$$

and β and γ play a role similar to the intrinsic collective variables in the Bohr Hamiltonian. The ground-state energy surface is obtained as the expectation value of the boson Hamiltonian (2.1) in the intrinsic state, i.e.,

$$E_{\text{g.s.}}(\beta,\gamma) = \langle \Phi_{\text{g.s.}}(\beta,\gamma) | H_B | \Phi_{\text{g.s.}}(\beta,\gamma) \rangle. \tag{2.7}$$

In a similar way, one introduces the intrinsic state associated with the β band by

$$\Phi_\beta(\beta,\gamma) = \frac{1}{\sqrt{(N-1)!}} (b^\dagger_{\text{g.s.}}(\beta,\gamma))^{N-1} b^\dagger_\beta(\beta,\gamma)|0\rangle, \tag{2.8}$$

where the basic β boson is given by [3,15]

$$b^\dagger_\beta(\beta,\gamma) = \frac{1}{\sqrt{1+\beta^2}} \left(-\beta s^\dagger + \cos\gamma d^\dagger_0 + \frac{1}{\sqrt{2}} \sin\gamma (d^\dagger_2 + d^\dagger_{-2}) \right). \tag{2.9}$$

The energy of the β band is obtained as the expectation value of the boson Hamiltonian (2.1) in the intrinsic β state, i.e.,

$$E_\beta(\beta,\gamma) = \langle \Phi_\beta(\beta,\gamma) | H_B | \Phi_\beta(\beta,\gamma) \rangle. \tag{2.10}$$

Within the intrinsic frame formalism, one can also calculate wave functions with the correct quantum numbers by projecting with the proper kernels. In correspondence to each intrinsic state, one has in the laboratory frame a band-like structure. Since the intrinsic system is γ dependent, the proper kernels connecting intrinsic and laboratory frames are given by the functions $\Psi_{\tau,L,M}(\gamma,\theta_i)$ [16], characterized by the quantum numbers (τ, L, M), solutions of the γ-angular part of the Bohr Hamiltonian with γ-independent potential. These functions can be viewed as a sort of generalization to five dimensions of the usual three-dimensional D functions,

$$\left(-\frac{1}{\sin 3\gamma} \frac{\partial}{\partial\gamma} \sin 3\gamma \frac{\partial}{\partial\gamma} + \frac{1}{4} \sum_{k=1}^{3} \frac{Q_k^2}{\sin^2\left(\gamma - \frac{2}{3}\pi k\right)} \right) \times \Psi_{\tau,L,M}(\gamma,\theta_i) = \tau(\tau+3) \Psi_{\tau,L,M}(\gamma,\theta_i), \tag{2.11}$$

where θ_i stands for the three Euler angles, and the Q_κ's are the components of the angular momentum written in terms of the Euler angles. The resulting spectrum (with degeneracies and energies) is the one characterizing the O(5) symmetry. In our context, the only relevant functions are those with zero component of the angular momentum. To simplify the notation, we shall henceforth drop from the labels in Ψ the index corresponding to $M = 0$. As an example, we quote here the explicit form of the function associated with the 2^+ state with $\tau = 1$,

$$\Psi_{1,2}(\gamma,\theta,\phi) = (1/\sqrt{8\pi}) \{ \cos\gamma Y_{20}(\theta,\phi) + (1/\sqrt{2}) \times \sin\gamma [Y_{22}(\theta,\phi) + Y_{2-2}(\theta,\phi)] \}. \tag{2.12}$$

As a result all the members of the ground-state and the β band are described by the wave functions

$$|\tau, L\rangle_{\text{g.s.}} = \Psi_{\tau L}(\gamma, \theta_i)|\Phi_{\text{g.s.}}(\beta_{\min}, \gamma)\rangle, \tag{2.13}$$

and

$$|\tau, L\rangle_{\beta} = \Psi_{\tau L}(\gamma, \theta_i)|\Phi_{\beta}(\beta_{\min}, \gamma)\rangle, \tag{2.14}$$

in terms of the intrinsic states $\Phi_{\text{g.s.}}(\beta_{\min}, \gamma)$ and $\Phi_{\beta}(\beta_{\min}, \gamma)$. The evaluation of matrix elements associated with transition rates will involve an integration over the variables γ and the Euler angles plus the matrix element in the intrinsic frame. The $B(E\lambda)$ values within two given states in bands a and b, respectively, can be evaluated according to

$$\begin{aligned} B(E\lambda; (\tau_i, L_i)_a \rightarrow (\tau_f, L_f)_b) &= \frac{1}{2L_i + 1} |_b\langle \tau_f L_f || \widehat{T}^{(E\lambda)}(\text{lab}) || \tau_i L_i \rangle_a|^2 \\ &= \frac{1}{2L_i + 1} \begin{pmatrix} L_i & \lambda & L_f \\ 0 & 0 & 0 \end{pmatrix}^{-2} \\ &\quad \times |\langle \Psi_{\tau_i, L_i}(\gamma, \theta, \phi)| \widehat{T}^{(E\lambda)}_{ab}(\text{intr})(\gamma, \theta, \phi) |\Psi_{\tau_f, L_f}(\gamma, \theta, \phi)\rangle|^2. \end{aligned} \tag{2.15}$$

The formalism presented so far for the β band is strictly valid only when the energy surface admits a value of $\beta_{\min} \neq 0$. In the case of Hamiltonian (2.1), this only happens along the O(6) side of the phase transition. When $\beta_{\min} = 0$ [the U(5) side], the coherent states in Eqs. (2.5) and (2.6) are still valid, but they become just a condensate of s bosons. On the other hand, with $\beta_{\min} = 0$, the one-phonon excitation state obtained from Eqs. (2.8) and (2.9) becomes a pure $L = 2$ state (admixture of d bosons), and therefore it cannot contain an $L = 0$ state. This must be searched within the two-phonon triplet whose structure is

$$(s^{\dagger})^{N-2} \left(\cos\gamma d^{\dagger}_0 + \frac{1}{\sqrt{2}} \sin\gamma (d^{\dagger}_2 + d^{\dagger}_{-2}) \right)^2 |0\rangle. \tag{2.16}$$

In the next section, results obtained within this formalism for selected transitions will be compared against the exact results for the complete transitional O(6)–U(5) line. The operator used for $E2$ transitions is equal to $\hat{Q}^{\text{lab}}$ of Ref. [17] with $\chi = 0$, while for $E0$ transitions, it is $T^{(E0)}(\text{lab}) = \widehat{n}_s$.

III. RESULTS FOR THE U(5)–O(6) TRANSITIONAL REGION

In this section, we compare exact calculations for the energies, $B(E2)$'s, and $B(E0)$'s with the approximate ones obtained within the CS approach.

A. Excitation energies

To show the shape phase transition, we present in Fig. 2 exact calculations, as a function of the control parameter x, for the excitation energies of the first 2^+ in the ground-state band (upper panel) and for the excitation energy of the bandhead of the β band (lower panel) for different values of N ($N = 10, 100, 1000$). For $x = 0$ [i.e., in the O(6) symmetry], the 0^+_{β}

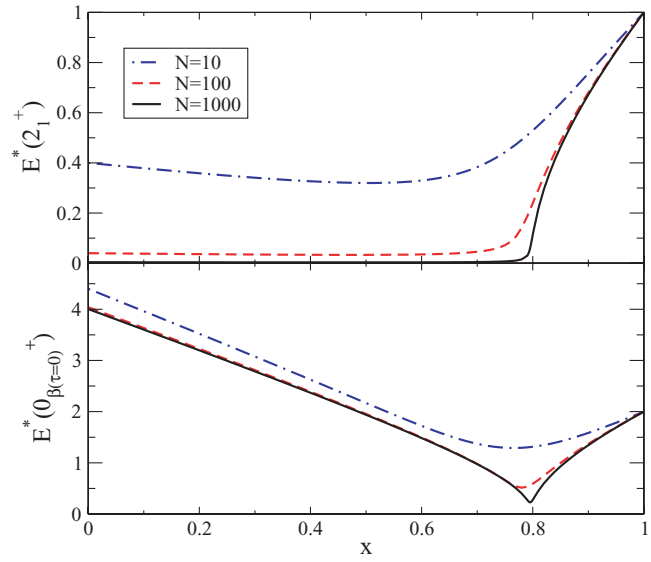

FIG. 2. (Color online) Excitation energies for the 2^+_1 (gap Δ) and for the second 0^+ with v or $\tau = 0$. Exact calculations are presented for $N = 10$, 100, and 1000.

state (i.e., the bandhead of the β band) has quantum numbers $\sigma = N - 2$ and $\tau = 0$ and is known to have excitation energy $E_{\beta} = 4 + 4/N$. At the other extreme (the spherical limit), the β bandhead transforms into the two-phonon state 0^+ and, consequently, has an excitation energy of 2. Concerning the gap (Δ) (excitation energy of the first excited state), for the Hamiltonian (2.1) it goes as $\tau(\tau + 3)/N = 4/N$ in the O(6) limit and tends to zero as N goes to infinity. In the large N limit, Δ is zero in the deformed phase and different from zero in the spherical one. In the U(5) limit, $\Delta = 1$ (one-phonon state). The transition is clearly observed in the behavior of Δ and is sharper as N increases.

To compare these results with those provided by the CS approach, we used Eq. (2.7) and our boson Hamiltonian (2.1) to provide the ground-state energy surface:

$$E_{\text{g.s.}}(\beta, \gamma) = \frac{Nx\beta^2}{1 + \beta^2} - (1 - x)\left(\frac{4(N - 1)\beta^2}{(1 + \beta^2)^2} + \frac{5 + \beta^2}{1 + \beta^2} \right). \tag{3.1}$$

In our specific case, as expected from the overall O(5) symmetry, the energy surfaces for any value of the control parameter x are completely γ independent. As far as the β dependence is concerned, for x values larger than the critical $x_c = \frac{4N-8}{5N-8}$, the system finds more convenient a spherical shape ($\beta_{\min} = 0$); whereas for x values smaller than x_c, the minimum corresponds to a deformed value

$$\beta_{\min}(N, x) = \sqrt{\frac{8(1 - x) + N(5x - 4)}{N(3x - 4)}}. \tag{3.2}$$

At the critical point x_c, the energy surface ends up being rather flat around the origin as is expected for a second-order phase transition [9].

For the β band (when $x < x_c$), the corresponding energy surface, Eq. (2.10), again γ independent, is given by

$$E_\beta(\beta,\gamma) = \frac{x(1+(N-1)\beta^2)}{1+\beta^2} + (x-1) \times \frac{4N^2\beta^2 + N(7-18\beta^2+3\beta^4) + 2(\beta^4+10\beta^2-3)}{N(1+\beta^2)^2}. \tag{3.3}$$

The predicted excitation energy of the β band is therefore given by

$$E^*_\beta = E_\beta(\beta,\gamma) - E_{\text{g.s.}}(\beta,\gamma) = x\frac{1-\beta^2}{1+\beta^2} - 2(1-x) \times \frac{N(\beta^4-10\beta^2+1)+\beta^4+10\beta^2-3}{N(1+\beta^2)^2}. \tag{3.4}$$

Note that for $x = 0$, i.e., for the O(6) case, for large N the value of the minimum approaches $\beta_{\min} = 1$ and the excitation energy becomes $E^*_\beta = 4 - 4/N$ to be compared with the exact value $4 + 4/N$, i.e., with a discrepancy of the order of $1/N$. For the other values of x the resulting excitation energies are given in Fig. 3 in comparison with the results obtained in the exact calculation for different N values.

As mentioned above, the β band in the intrinsic frame is only defined for the deformed region, $\beta_{\min} \neq 0$. In the spherical phase [the U(5)-side of the phase transition], the first excited 0^+ is among the two-phonon triplet. The energy of these states is calculated to be

$$E_{0_2^+} = 11x - 9 + (1-x)\frac{16}{N}. \tag{3.5}$$

Since for the ground state Eq. (3.1) can be used with $\beta = 0$, the excitation energy of the first excited 0^+ state in the spherical phase is given by

$$E^*_{0_2^+} = 6x - 4 + (1-x)\frac{16}{N}. \tag{3.6}$$

In Fig. 3, these results are plotted for the spherical phase ($x > x_c$).

From Fig. 3, it is observed that the agreement all along the transitional region is of the order $1/N$, as in the limits. Larger discrepancies are obtained close to the critical point.

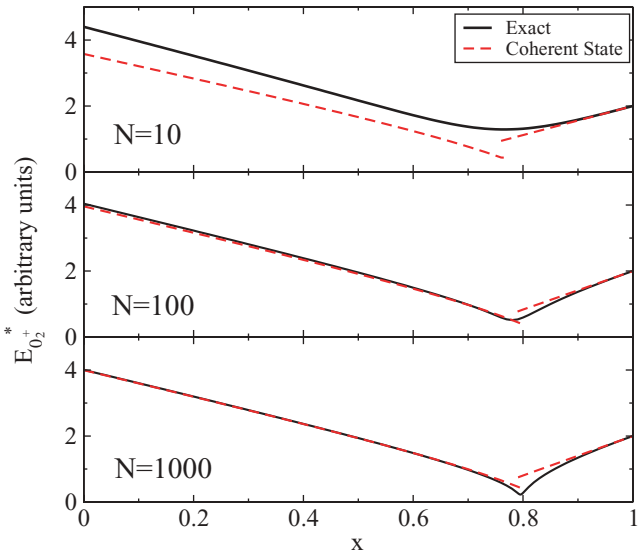

FIG. 3. (Color online) Excitation energies for the 0^+_2 state. In the intrinsic frame, this corresponds to (a) the β band for the deformed phase [$0 < x < x_c$ with $x_c = (4N-8)/(5N-8)$] and (b) the 0^+ in the two-phonon triplet for the spherical phase ($x_c < x < 1$). In the exact calculation, the plotted energy corresponds to the second 0^+ state with $v = 0$ (or $\tau = 0$), which corresponds to the bandhead of the β band in the O(6) region, while it is the two-phonon state in the U(5) region. Exact calculations and approximate CS calculations are presented for $N = 10$, l00, and 1000.

B. $E2$ and $E0$ transition probabilities

Apart from the energies one can calculate, as a function of x and both for exact and approximate CS approaches, the value of the intraband $B(E2)$ matrix elements within the ground and β bands $B(E2; 2^+_g \to 0^+_g)$, $B(E2;4^+_g \to 2^+_g)$, and $B(E2;2^+_\beta \to 0^+_\beta)$ and the interband values $B(E2;0^+_\beta \to 2^+_g)$.

In the intrinsic state formalism, following Eq. (2.15), the $B(E2)$ values within the ground band can be evaluated according to

$$B(E2;(\tau_1,L_1)_g \to (\tau_2,L_2)_g) = \frac{1}{2L_1+1}|{}_g\langle\tau_1 L_1||\widehat{Q}^{\text{lab}}||\tau_2 L_2\rangle_g|^2 = \frac{1}{2L_1+1}\begin{pmatrix} L_1 & 2 & L_2 \\ 0 & 0 & 0\end{pmatrix}^{-2} \times |\langle\Psi_{\tau_1,L_1}(\gamma,\theta,\phi)|\widehat{Q}^{\text{intr}}_{gg}(\gamma,\theta,\phi)|\Psi_{\tau_2,L_2}(\gamma,\theta,\phi)\rangle|^2, \tag{3.7}$$

where the intrinsic quadrupole moment is

$$\widehat{Q}^{\text{intr}}_{gg}(\gamma,\theta,\phi) = \langle\Phi_{\text{g.s.}}|\widehat{Q}^{\text{lab}}_0|\Phi_{\text{g.s.}}\rangle = \langle\Phi_{\text{g.s.}}|\sum_\mu \sqrt{\frac{4\pi}{5}}(-1)^\mu \widehat{Q}_\mu Y_{2,\mu}(\theta,\phi)|\Phi_{\text{g.s.}}\rangle, \tag{3.8}$$

which can be evaluated giving

$$Q^{\text{intr}}_{gg}(\gamma,\theta,\phi) = \sqrt{\frac{4\pi}{5}}\frac{2\beta}{1+\beta^2}N\{\cos\gamma\, Y_{20}(\theta,\phi) + (1/\sqrt{2})\sin\gamma[Y_{22}(\theta,\phi)+Y_{2-2}(\theta,\phi)]\} = 8\pi N\sqrt{\frac{2}{5}}\frac{\beta}{1+\beta^2}\Psi_{1,2}(\gamma,\theta,\phi). \tag{3.9}$$

This leads to the final value for the transition from 2^+_g ($\tau = 1$) to 0^+_g ($\tau = 0$)

$$B(E2;2^+_g \to 0^+_g) = N^2\frac{4\beta^2}{5(1+\beta^2)^2}, \tag{3.10}$$

and similarly for the transition from the 4_g^+ ($\tau = 2$) to the 2_g^+ ($\tau = 1$) state

$$B(E2; 4_g^+ \to 2_g^+) = N^2 \frac{8\beta^2}{7(1+\beta^2)^2}. \quad (3.11)$$

Use has been made of the recursion relation

$$\begin{aligned}\Psi_{1,2}(\gamma,\theta,\phi) \times \Psi_{1,2}(\gamma,\theta,\phi) &= \frac{\sqrt{2}}{8\pi}\Psi_{0,0}(\gamma,\theta,\phi) + \frac{1}{7\pi}\sqrt{\frac{5}{8}}\Psi_{2,2}(\gamma,\theta,\phi) \\ &+ \frac{3}{14\pi\sqrt{2}}\Psi_{2,4}(\gamma,\theta,\phi), \end{aligned} \quad (3.12)$$

for the evaluation of the matrix elements involving the Ψ functions.

In a similar way, we can determine the intensities within the β band and the interband transitions. For the transition within the β band, one needs to evaluate the intrinsic quadrupole matrix element in the β band, i.e.,

$$\begin{aligned} Q^{\rm intr}_{\beta\beta}(\gamma,\theta,\phi) &= \langle\Phi_\beta|\widehat{Q}_0^{\rm lab}|\Phi_\beta\rangle \\ &= \langle\Phi_\beta|\sum_\mu \sqrt{\frac{4\pi}{5}}(-1)^\mu \widehat{Q}_\mu Y_{2,\mu}(\theta,\phi)|\Phi_\beta\rangle \\ &= \sqrt{\frac{4\pi}{5}}\frac{2\beta}{1+\beta^2}(N-2)\{\cos\gamma Y_{20}(\theta,\phi) \\ &\quad + (1/\sqrt{2})\sin\gamma[Y_{22}(\theta,\phi) + Y_{2-2}(\theta,\phi)]\} \\ &= 8\pi(N-2)\sqrt{\frac{2}{5}}\frac{\beta}{1+\beta^2}\Psi_{1,2}(\gamma,\theta,\phi), \end{aligned} \quad (3.13)$$

which leads, for example, to the transition probability from the state $2_\beta^+(\tau = 1)$ to $0_\beta^+(\tau = 0)$

$$B(E2; 2_\beta^+ \to 0_\beta^+) = (N-2)^2 \frac{4\beta^2}{5(1+\beta^2)^2}. \quad (3.14)$$

Finally, for the interband β-ground transitions, one has to calculate the nondiagonal quadrupole matrix elements between the intrinsic ground and β states:

$$\begin{aligned} Q^{\rm intr}_{g\beta}(\gamma,\theta,\phi) &= \langle\Phi_\beta|\widehat{Q}_0^{\rm lab}|\Phi_{\rm g.s.}\rangle \\ &= \langle\Phi_\beta|\sum_\mu \sqrt{\frac{4\pi}{5}}(-1)^\mu \widehat{Q}_\mu Y_{2,\mu}(\theta,\phi)|\Phi_{\rm g.s.}\rangle \\ &= \sqrt{\frac{4\pi}{5}}\sqrt{N}\frac{1-\beta^2}{1+\beta^2}\{\cos\gamma Y_{20}(\theta,\phi) \\ &\quad + (1/\sqrt{2})\sin\gamma[Y_{22}(\theta,\phi) + Y_{2-2}(\theta,\phi)]\} \\ &= 4\pi\sqrt{N}\sqrt{\frac{2}{5}}\frac{1-\beta^2}{1+\beta^2}\Psi_{1,2}(\gamma,\theta,\phi), \end{aligned} \quad (3.15)$$

which leads, for example, to the transition probability from the state $0_\beta^+(\tau = 0)$ to $2_g^+(\tau = 1)$

$$B(E2; 0_\beta^+ \to 2_g^+) = N\frac{(1-\beta^2)^2}{(1+\beta^2)^2}. \quad (3.16)$$

In all these equations, the shape variable β should be fixed to the value of $\beta = \beta_{\rm min}$ that minimizes the ground-state energy surface. In Fig. 4, the exact $B(E2)$'s for the transitions $2_g^+ \to 0_g^+, 4_g^+ \to 2_g^+, 2_\beta^+ \to 0_g^+$, and $0_\beta^+ \to 2_g^+$ are compared with the CS approximation for different N values. As a last comparison, in the last column, we also display the values of the $E0$ transition probabilities from the 0^+ of the β band to the ground-state 0^+. In the intrinsic frame formalism, this transition probability is given by

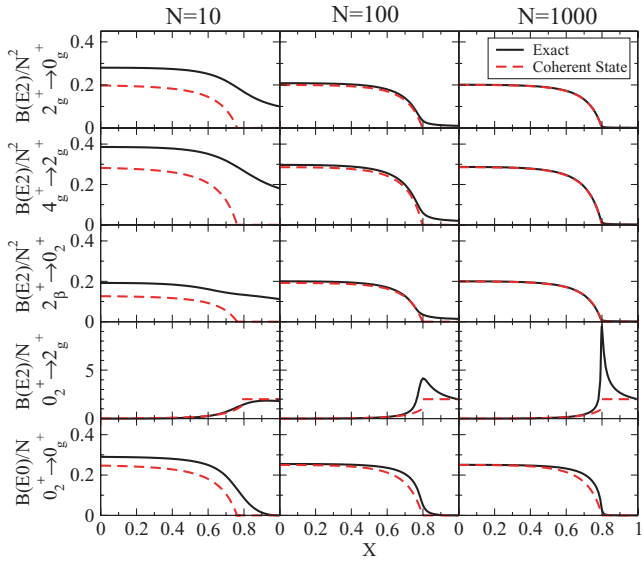

FIG. 4. (Color online) $B(E2)$ values for the transitions labeled on each row: $2_g^+ \to 0_g^+, 4_g^+ \to 2_g^+, 2_\beta^+ \to 0_2^+$, and $0_2^+ \to 2_g^+$. In each case exact and CS results are presented for $N = 10$, $N = 100$, and $N = 1000$. Coherent state results are plotted for the deformed and the spherical regions. In the deformed phase, the 0_2^+ state is the bandhead of the β band and 2_β stands for the first excited state of this band; in the spherical phase, the 0_2^+ state is the 0^+ in the two-phonon triplet and 2_β stands for the 2^+ in the three-phonon quintuplet. Each $B(E2)$ is divided by N^2 or N in order to use the same scale independently of the value of N. Please note the different scale for $B(E2; 0_2^+ \to 2_g^+)$. The last row displays the values of the $E0$ transition probability (divided by N) from the 0^+ of the β band (or two-phonon state) to the ground-state 0^+.

$$B(E0; 0_\beta^+ \to 0_g^+) = |\langle\Psi_{0,0}|\left(\widehat{n}_s^{\rm intr}\right)_{g\beta}|\Psi_{0,0}\rangle|^2, \quad (3.17)$$

where the intrinsic $\widehat{n}_s$ operator is

$$(\widehat{n}_s^{\rm intr})_{g\beta} = \langle\Phi_{\rm g.s.}|\widehat{n}_s^{\rm lab}|\Phi_{\rm g.s.}\rangle = -\sqrt{N}\frac{\beta}{1+\beta^2}. \quad (3.18)$$

This gives for the $B(E0)$,

$$B(E0; 0_\beta^+ \to 0_g^+) = N\frac{\beta^2}{(1+\beta^2)^2}. \quad (3.19)$$

The exact calculations for $B(E2)$ can be checked in the limits, since analytical expressions are known and given in Fig. 1. For the $E0$ case, the exact value of $B(E0; 0_\beta^+ \to 0_g^+)$ in the O(6) limit is calculated to be [3]

$$B^{(\rm O6)}(E0; 0_\beta^+ \to 0_g^+) = N\frac{(N+3)(N+2)(N-1)}{4N(N+1)^2}, \quad (3.20)$$

which, in the large N limit, goes to $N/4$. This $B(E0)$ is zero in the U(5) limit, since n_s is a good quantum number in this

limit, and then the operator $\widehat{n}_s$ does not induce transitions from 0^+_β to 0^+_g.

The CS results can be checked in the O(6) limit because results have already been reported [17]. In all cases, the critical point is clearly observed for large N, and, in this case, the CS approach provides a fairly good approximation to the exact results, except for very close to the critical point, where large discrepancies can be seen in $B(E2; 0^+_\beta \to 2^+_g)/N$. For small N values, discrepancies of the next-to-leading-order terms in the $1/N$ expansion are already observed in the deformed region. Larger deviations are observed close to the critical point. All along the U(5) quasidynamical symmetry region, the structure of the states (2.16), and therefore the $B(E2)$ values, coincides with the U(5) limit. With reference to Fig. (4), the asymptotic values for properly normalized $B(E2)$'s (in the limit of large N and for $x > x_c$) are 2 for the fourth row and 0 in all other cases.

IV. SUMMARY AND CONCLUSIONS

The degree of accuracy of the coherent state (CS) approach to the interacting boson model has been tested along the entire O(6)–U(5) transitional region. We have studied excitation energies of the β band and $B(E2)$ and $B(E0)$ transitions for selected intraband and interband transitions. For that purpose, the appropriate kernels to project from intrinsic to laboratory frames were used. In the spherical phase, the coherent state formalism can be used and gives reasonable results [exact in the U(5) limit] except close to the critical point. Consequently, we conclude that the CS formalism provides in all cases approximations to the exact results of the order $1/N$ in the transitional region except close to the critical point. Finite-N effects cannot be analyzed within the CS formalism, since next-to-leading-order terms are not correctly calculated.

ACKNOWLEDGMENTS

This work has been partially supported by the Italian-Spanish INFN-MCYT agreement, by the Spanish MEC, by the European regional development fund (FEDER) under projects FIS2008-04189 and CPAN-Ingenio, and by the Junta de Andalucía. I. Inci acknowledges the financial support of the Scientific and Technical Research Council of Turkey (TÜBİTAK), under project number TBAG-107T824 as well as the support of the Turkish Academy of Sciences (TÜBA-GEBİP).

[1] P. Cejnar and J. Jolie, Prog. Part. Nucl. Phys. **62**, 210 (2009).
[2] R. F. Casten, Prog. Part. Nucl. Phys. **62**, 183 (2009).
[3] F. Iachello and A. Arima, *The Interacting Boson Model* (Cambridge University Press, New York, 1987).
[4] J. N. Ginocchio and M. W. Kirson, Nucl. Phys. **A350**, 31 (1980).
[5] A. E. L. Dieperink, O. Scholten, and F. Iachello, Phys. Rev. Lett. **44**, 1747 (1980).
[6] A. Bohr and B. Mottelson, Phys. Scr. **22**, 468 (1980).
[7] A. Bohr and B. Mottelson, *Nuclear Structure* (Benjamin, Reading, MA, 1975), Vol. 2.
[8] F. Iachello, Phys. Rev. Lett. **85**, 3580 (2000).
[9] J. M. Arias, C. E. Alonso, A. Vitturi, J. E. García-Ramos, J. Dukelsky, and A. Frank, Phys. Rev. C **68**, 041302(R) (2003).
[10] J. E. García-Ramos, J. Dukelsky, and J. M. Arias, Phys. Rev. C **72**, 037301 (2005).
[11] S. Dusuel, J. Vidal, J. M. Arias, J. Dukelsky, and J. E. García-Ramos, Phys. Rev. C **72**, 011301(R) (2005).
[12] S. Dusuel, J. Vidal, J. M. Arias, J. Dukelsky, and J. E. García-Ramos, Phys. Rev. C **72**, 064332 (2005).
[13] J. Vidal, J. M. Arias, J. Dukelsky, and J. E. García-Ramos, Phys. Rev. C **73**, 054305 (2006).
[14] J. M. Arias, J. Dukelsky, J. E. García-Ramos, and J. Vidal, Phys. Rev. C **75**, 014301 (2007).
[15] A. Leviatan, Ann. Phys. (NY) **179**, 201 (1987).
[16] D. Bès, Nucl. Phys. **10**, 373 (1959).
[17] C. E. Alonso, M. Lozano, C. H. Dasso, and A. Vitturi, Phys. Lett. **B212**, 1 (1988).